G. Ertl

THE NOBEL PRIZE IN CHEMISTRY 2007

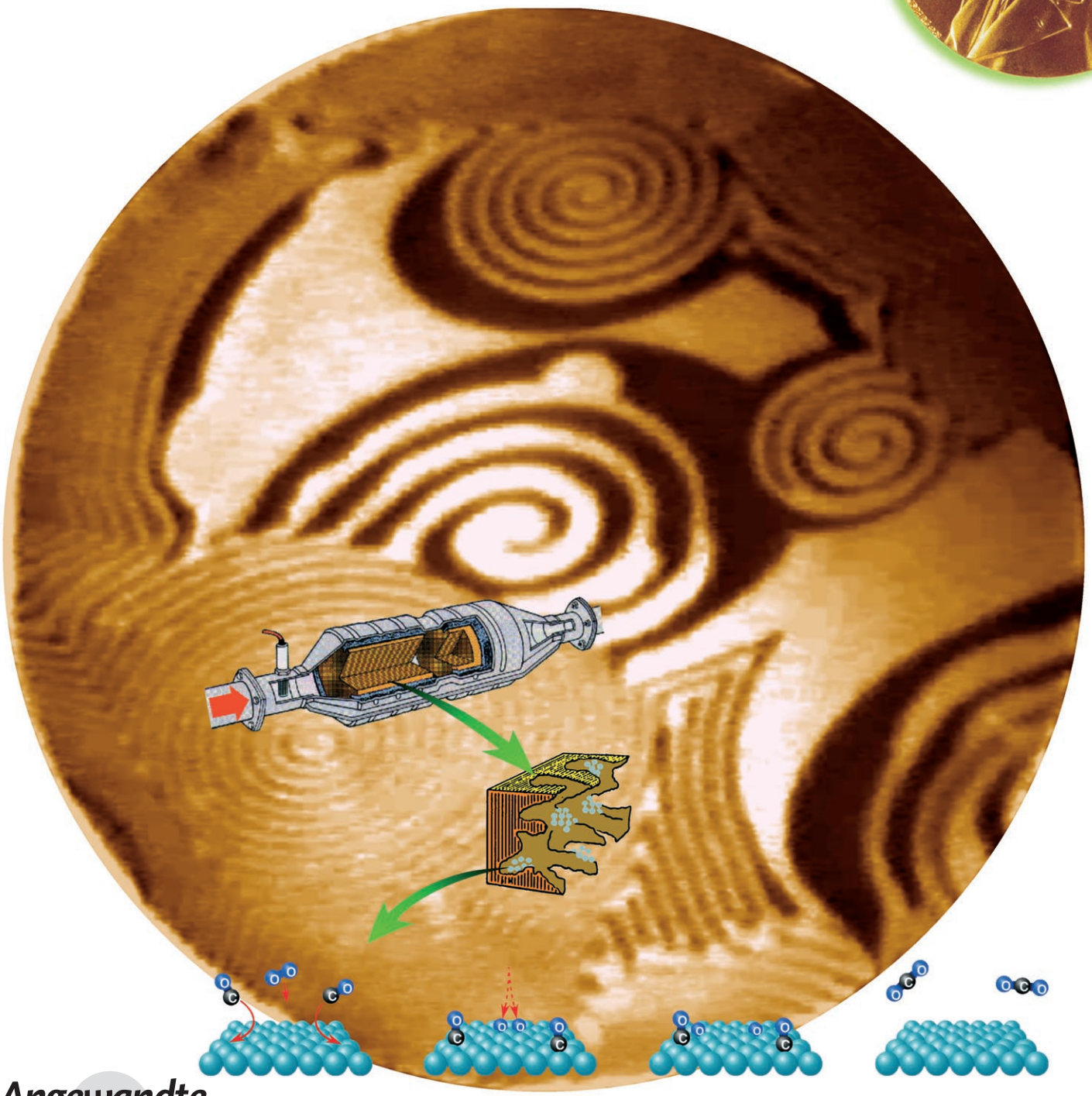

Angewandte Chemie

Angewandte Chemie

Heterogeneous Catalysis

DOI: 10.1002/anie.200800480

Reactions at Surfaces: From Atoms to Complexity (Nobel Lecture)**

*Gerhard Ertl**

Keywords:
ammonia synthesis · carbon monoxide · Nobel lecture · oscillating reactions · surface chemistry

From the Contents

1. Introduction

The secretary of the Royal Swedish Academy of Sciences, the famous chemist Jöns Jacob Berzelius, published since 1820 annual review articles on the most significant new developments in his field. Since the early 19th century there were observations from several laboratories that certain substances influenced the progress of a chemical reaction without being consumed and hence apparently not being affected by this reaction. For example, Johann Wolfgang Döbereiner, professor of chemistry at the University of Jena, reported in July 1823 to his minister, Johann Wolfgang von Goethe, "*that finely divided platinum powder causes hydrogen gas to react with oxygen gas by mere contact to water whereby the platinum itself is not altered*".[1][***] In his report published in 1835, Berzelius defined this phenomenon as "catalysis", rather in order to introduce a classification than to offer a possible explanation.[2] Throughout the rest of this century, the term catalysis remained heavily debated[3] until around 1900 Wilhelm Ostwald proposed its valid definition in terms of the concepts of chemical kinetics: "*A catalyst is a substance which affects the rate of a chemical reaction without being part of its end products*".[4][****] In 1909, Ostwald was awarded the Nobel Prize in Chemistry for his contributions to catalysis.

A chemical reaction involves breaking of bonds between atoms and the formation of new ones. This process is associated with transformation of energy, and the energy diagram illustrating the progress of a reaction $A+B \rightarrow C$ is depicted schematically in Figure 1. The activation energy E^* to be surmounted is usually provided by thermal energy kT,

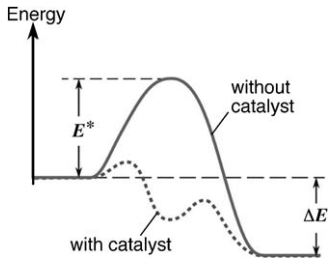

Figure 1. Energy diagram illustrating the progress of a chemical reaction with and without a catalyst.

with k being Boltzmann's constant and T the temperature, and accordingly not all molecular encounters will be successful, but only a fraction $e^{-E^*/kT}$. An increase of the reaction probability (= rate) can be achieved by either increasing the

[*] Prof. Dr. G. Ertl
Fritz-Haber-Institut der Max-Planck-Gesellschaft
14195 Berlin (Germany)
Fax: (+49) 30-8413-5106
E-mail: ertl@fhi-berlin.mpg.de

Supporting information for this article is available on the WWW under http://www.angewandte.org or from the author.

[***] "*daß das rein metallische staubfeine Platin die höchst merkwürdige Eigenschaft hat, das Wasserstoffgas durch bloße Berührung zu bestimmen, daß es sich mit Sauerstoffgas zu Wasser verbindet*"

[****] "*Ein Katalysator ist jeder Stoff, der, ohne im Endprodukt einer chemischen Reaktion zu erscheinen, ihre Geschwindigkeit verändert.*"

temperature or by lowering the activation energy E^*. The latter is provided by the catalyst, which through the formation of intermediate compounds with the molecules involved in the reaction provides an alternate reaction path as sketched by the dashed line in Figure 1 which is associated with smaller activation barriers and hence a higher overall reaction rate. In the last step, the product molecules are released from the catalyst, which is now available for the next reaction cycle. If the reacting molecules and the catalyst are in the same (gaseous or liquid) phase, the effect is called homogeneous catalysis. In living systems, macromolecules (= enzymes) play the role of catalysts. In technical reactions, mostly the interaction of molecules with the surface of a solid is decisive. The principle of this heterogeneous catalysis is depicted schematically in Figure 2.

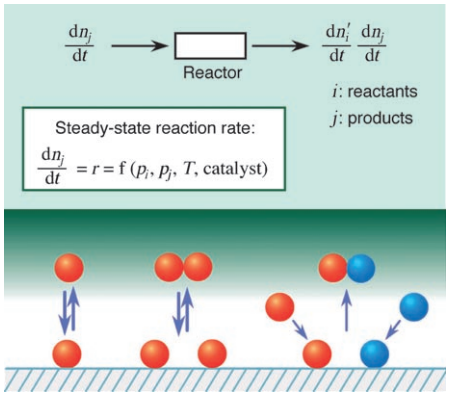

Figure 2. The principle of heterogeneous catalysis.

The atoms in the surface layer of a solid have fewer neighbors than those in the bulk and are hence chemically unsaturated and may form new bonds (= chemisorption) with suitable molecules impinging from the adjacent gas or liquid phase. By this step, existing bonds will be modified or may even be broken (= dissociative chemisorption). The surface species formed may jump from one site to neighboring ones, then may react with others, and the formed produced molecules eventually leave the surface (= desorption). If operated in a flow reactor, the catalyst can in this way continuously operate without being consumed.

One of the first and still most important technical applications of this principle was realized about 100 years ago: Owing to the continuous increase of the world population and exhaustion of the natural supply of nitrogen fertilizers, the world was facing a global threat of starvation. As Sir William Crookes, president of the British Association for the Advancement of Science, formulated it:[5] "... *all civilized nations stand in deadly peril of not having enough to eat ... the fixation of atmospheric nitrogen is one of the great discoveries awaiting the ingenuity of chemists*".

Nitrogen fixation means transformation of the abundant N_2 molecule (which constitutes about 80 % of our air) from its state of very strong bond between the two N atoms into a more reactive form according to the reaction $N_2 + 3H_2 \rightarrow 2NH_3$. This reaction of ammonia formation could be realized in 1909 by Fritz Haber (Nobel Prize 1919) in the laboratory by the use of an osmium catalyst in a high-pressure flow apparatus.[6] Carl Bosch (Nobel Prize 1931) from the BASF company started immediately to develop this method into a technical process, and the first industrial plant started operation in 1913, only a few years later. Figure 3 shows the growth of the world population together with the ammonia production over the last century,[7] and it is quite obvious that our present life would be quite different without the development of the Haber–Bosch process.

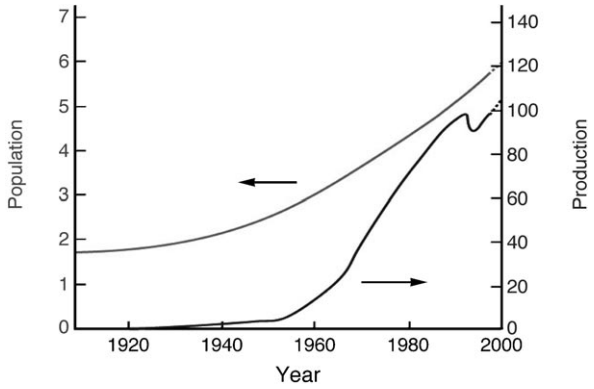

Figure 3. Variation of the world population (in 10^9) and the ammonia production (in 10^6 metric tons of nitrogen) during the 20th century.[7]

However, large-scale technical production would not have been possible without the availability of large quantities of a cheap catalyst. (The complete world supply of the precious metal osmium was only 80 kg in those days.) This task could be solved successfully by Alwin Mittasch[8] who in thousands of tests found that a material derived from a Swedish iron ore exhibited satisfactory activity. This type of doubly promoted iron catalyst is in fact still in use today in almost all industrial plants.

Remarkably, despite the enormous technical significance of the Haber–Bosch reaction and despite of numerous laboratory studies, its actual mechanism remained unclear over many years. P. H. Emmett, one of the pioneers of

Gerhard Ertl was born in 1936. He studied physics at the University of Stuttgart and received his PhD in physical chemistry in 1965 from the Technical University of Munich under the supervision of Heinz Gerischer in the field of electrochemistry. In 1968 he became professor of physical chemistry at the Technical University of Hanover, in 1973 he moved to the Ludwig Maximilians University of Munich, and in 1986 he became the successor of his PhD advisor as director of the Fritz Haber Institute. At the same time he became honorary professor at the Technical University of Berlin and the Free University of Berlin; in 1992 the Humboldt University of Berlin also awarded him this title. Among his many other awards are the Wolf Prize in Chemistry (1998), the Japan Prize of the Science and Technology Foundation of Japan (1992), and the Karl Ziegler Prize of the German Chemical Society (Gesellschaft Deutscher Chemiker, GDCh, 1998).

catalysis research, was honored in 1974 by a symposium at which he concluded:[9] "*The experimental work of the past 50 years leads to the conclusion that the rate-limiting step in ammonia synthesis over iron catalysts is the chemisorption of nitrogen. The question as to whether the nitrogen species involved is molecular or atomic is still not conclusively resolved …*".

2. The Surface Science Approach to Heterogeneous Catalysis: Ammonia Synthesis

The problem involved in the study of the surface chemistry of "real" catalysts becomes evident if we look on an electron micrograph of the Mittasch catalyst as reproduced in Figure 4:[10] A catalyst with high activity has to exhibit a

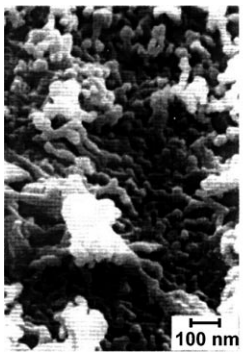

Technical conditions: $T \approx 400°C$, $p \approx 300$ bar
promoted iron catalyst

BASF S6-10 catalyst [at. %]

	Fe	K	Al	Ca	O
Bulk composition	40.5	0.35	2.0	1.7	53.2
Surface –					
unreduced	8.6	36.2	10.7	4.7	40.0
reduced	11.0	27.0	17.0	4.0	41.0
cat. active spot	30.1	29.0	6.7	1.0	33.2

Figure 4. Surface topography and chemical composition of an industrial ammonia synthesis catalyst.[10]

rather high specific surface area, which in this case is about 20 $m^2 g^{-1}$ as reflected by nanometer-sized active particles. (In fact, catalysis has been a nanotechnology long before this term was introduced.) Under reaction conditions, these particles are reduced into metallic iron covered by a submonolayer of K(+O), which acts as an "electronic" promoter. The configuration of active particles is stabilized against sintering by a framework of Al_2O_3 (and CaO); these compounds act as "structural" promoters. The active component itself will expose different crystal planes apart from various defects, and all these various structural parameters are expected to exhibit varying reactivity. Moreover, the question arises: how can the two-dimensional chemistry taking place in the chemisorbed overlayer be investigated on the atomic scale?

A possible strategy to overcome this problem had been suggested by Irving Langmuir (Nobel Prize 1932) already many years ago:[11] "*Most finely divided catalysts must have structures of great complexity. In order to simplify our theoretical consideration of reactions at surfaces, let us confine our attention to reactions on plane surfaces. If the principles in this case are well understood, it should then be possible to extend the theory to the case of porous bodies. In general, we should look upon the surface as consisting of a checkerboard …*"

The "surface science" approach that Langmuir had in mind was experimentally not yet accessible in his days, but began to become only available during the 1960s with the advent of ultrahigh vacuum (UHV) and surface sensitive physical methods.[12] Nowadays a whole arsenal of such techniques is available to study the structural, electronic, or dynamic properties of such well-defined single-crystal surfaces.

Bond-breaking upon chemisorption is perhaps the most important role of a catalyst. Figure 5 shows schematically the

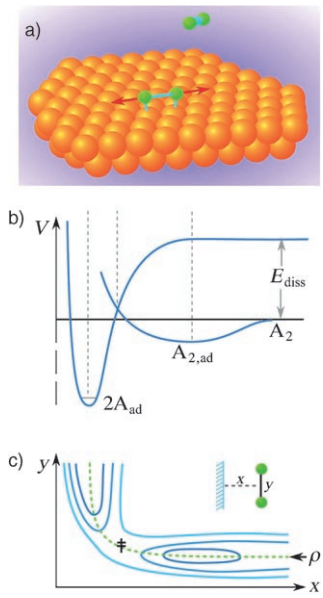

Figure 5. a) Illustration of the process of dissociative chemisorption of a diatomic molecule; b) one-dimensional Lennard–Jones diagram; c) two-dimensional representation of equipotential lines as function of the distance x of the molecule from the surface and the separation y between the two atoms.

energetic transformations in such a process if a diatomic molecule interacts with a perfect surface. Upon approaching the surface, the molecule may initiate the formation of new bonds to the surface atoms whereby the bond between the two atoms is weakened. A corresponding one-dimensional energy diagram as proposed by Lennard-Jones[13] is depicted in Figure 5b: If the molecule A_2 forms a bond with the surface, a shallow minimum ($A_{2,ad}$) is reached. If instead the free A_2 molecule dissociates, the dissociation energy E_{diss} is needed. Chemisorption of two A atoms would be associated with strong bond formation ($2A_{ad}$), and the crossing point between the two curves marks the activation energy for dissociative chemisorption, namely, the reaction $A_2 \rightarrow 2A_{ad}$. Even more instructive is a two-dimensional diagram (Figure 5c), in which lines of equal energy are plotted as a function of the distance x between the molecule and the surface and the separation y between the two atoms. (A full multidimensional description would require knowledge of the energy also as function of the point of impact within the unit cell of the surface as well as of the orientation of the molecular axis, and theory is nowadays able to provide this

information as well as on the dynamics of energy transfer between the different degrees of freedom.[14])

Figure 6 shows a scanning tunneling microscope (STM) picture from a Pt(111) surface with atomic resolution after

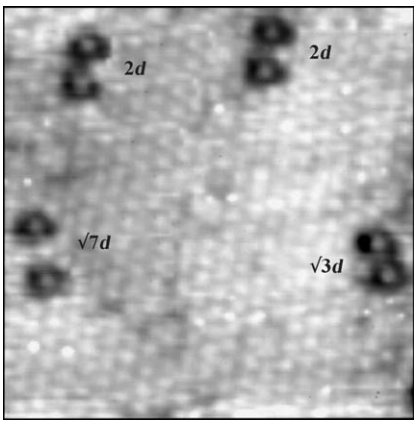

Figure 6. STM image from a Pt(111) surface (5.3×5.5 mm) after exposure to a small concentration of O_2 molecules at 165 K.[15]

exposure to a small amount of O_2 molecules at 165 K.[15] Apart from the Pt atoms from the topmost layer, additional features, namely pairs of bright dots surrounded by dark rings, are visible. The dots mark the positions of O atoms resulting from dissociative chemisorption. Whereas at 120 K chemisorbed O_2 molecules are discernible, at 165 K the thermal energy suffices to overcome the activation barrier for dissociation. The dark rings around the bright spots reflect the modification of the local electronic structure near the chemisorbed species. As a consequence, neighboring particles interact with each other through the electronic system of the substrate, whereby these interactions may be repulsive as well as attractive.[16] At the low temperature of 165 K, on the other hand, the chemisorbed O atoms are immobile and rest at those sites at which transfer of the chemisorption energy to the solid has been completed. This process requires a certain relaxation time during which the two separating O atoms move apart from each other, which is why two O atoms are never on neighboring sites, but are typically separated by 0.5–0.8 nm from each other. Taking into account the chemisorption energy released leads to an estimate of about 3×10^{-13} s for the lifetime of these "hot" adatoms.

More detailed insight into the dynamics of energy exchange between the solid and chemisorbed species can be obtained by application of ultrafast (femtosecond) laser techniques, and it can be generally concluded that with metal surfaces complete thermal equilibrium between all degrees of freedom is typically reached after about 10^{-12} s.[17]

The mean residence time of a chemisorbed particle on its momentary adsorption site is given by $\tau=\tau_0 e^{E^*_{diff}/kT}$, whereby E^*_{diff} is the activation energy for surface diffusion to a neighboring site. (E^*_{diff} is always much smaller than the adsorption energy, so that the adparticle makes many jumps before it eventually desorbs into the gas phase.) Figure 7a shows a snapshot taken with a fast STM from a Ru(0001) surface at 300 K covered by a small concentration of O atoms.

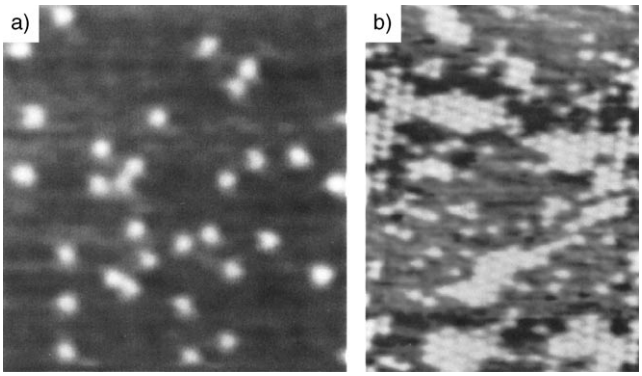

Figure 7. STM snapshots from O atoms adsorbed on a Ru(001) surface at 300 K:[18] a) at very small coverage; b) at higher coverage. A short movie showing the motion of the O atoms in real time is presented in the Supporting Information.

The latter jump around like with two-dimensional Brownian motion with a mean τ of about 6×10^{-2} s. However, τ varies with the mutual separation between two neighboring O atoms because of the operation of the above mentioned interactions and reaches about 0.22 s if the two O atoms are separated from each other by 2 lattice constants.[19] As a consequence of the operation of these weak attractive interactions, at higher surface concentrations the adsorbed particles are no longer uniformly and randomly distributed across the surface, but segregate into two phases as shown in Figure 7b: A two-dimensional quasi-crystalline phase is in equilibrium with a quasi-gas phase, where continuous nucleation, condensation, and sublimation occur like in analogous solid–gas equilibria. Such observations also reveal that the definition of a surface diffusion coefficient for adsorbates is meaningful only at low surface concentrations as long as the adsorbed particles can be considered to be independent from each other.[20]

The formation of ordered adsorbate phases with long-range periodicity such as in Figure 7b is quite common and permits determination of the actual structural parameters by a diffraction technique, preferably low-energy electron diffraction (LEED).[12] If we now return to the original problem of ammonia synthesis, dissociative chemisorption of nitrogen on various Fe single-crystal surfaces causes indeed also the formation of such structures derived from chemisorbed N atoms, such as reproduced in Figure 8 for the c2×2-N phase on the Fe(100) surface.[21] The probability for this process (= sticking coefficient) is very low, typically of the order 10^{-6}, which reflects the fact that this step is indeed rate-limiting in the overall reaction of ammonia synthesis. Figure 9 shows the variation of the surface concentration y (in relative units) of N atoms chemisorbed on various Fe single-crystal surfaces with exposure (i.e. number of molecules impinging per cm^2 and s) to N_2 gas at 693 K.[22] There is a pronounced influence of the surface structure: The most densely packed (110) surface is least active, whereas the open (111) plane exhibits the highest sticking coefficient and is indeed also responsible for the overall activity of the industrial catalyst.[23] This activity is further enhanced by the presence of the electronic promoter potassium, which stabilizes the intermediate $N_{2,ad}$ complex and hence increases its dissociation

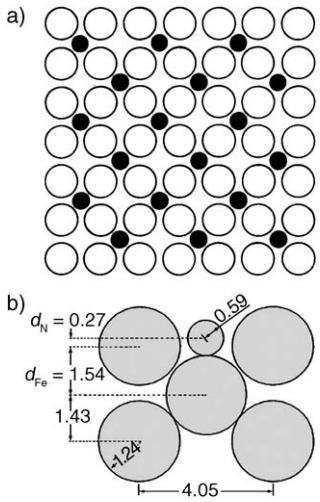

Figure 8. The structure of N atoms chemisorbed on a Fe(100) surface:[21] a) top view; b) side view. The distances are given in Å (1 Å = 10 nm).

probability.[24] The same sequence in reactivity as found for the sticking coefficient for dissociative nitrogen adsorption under low-pressure conditions was also found for the yield of ammonia production at a pressure of 20 bar.[25] Thus, it is also demonstrated that in this case there exists no "pressure gap".

All further steps involved in the ammonia synthesis reaction could be identified and analyzed similarly, so that the overall mechanism and energy diagram reproduced in Figure 10 could be derived.[26] This diagram exhibits the general features of the schematic diagram of Figure 1: Instead of overcoming the prohibitively high energy barrier for dissociation of the reacting molecules, the catalyst offers an alternate reaction path through formation of intermediate chemisorption complexes whose energy differences can be readily surmounted by the available thermal energy.

The kinetic parameters associated with the individual reaction steps can be put together to calculate the steady-state yield of ammonia formation for given external parameters. Figure 11 shows a plot of the ammonia yield derived on the basis of this kinetic model as a function of the experimental yields in industrial plants.[27] The data points barely deviate from the straight line marking complete agreement between theory and experiment. This result could be confirmed also by others[28] and demonstrates that in this case the "surface science" approach is indeed able to lead even to a quantitative description of an industrial reaction of great relevance.

3. Self-Organisation and Complexity: Oxidation of Carbon Monoxide

One of the major applications of heterogeneous catalysis in our days concerns protection of the environment through removal of toxic substances from car exhausts. Oxidation of

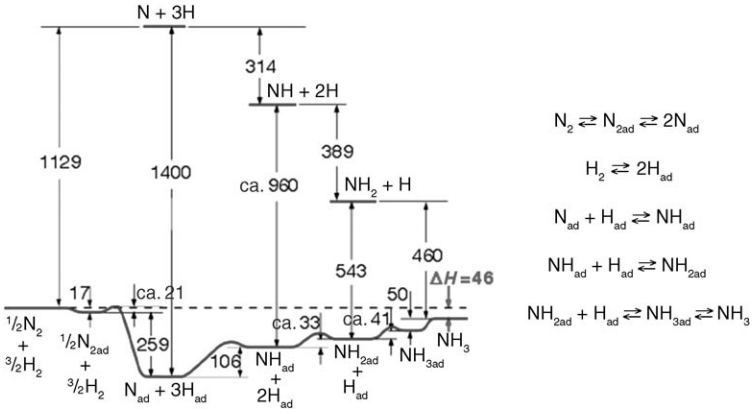

Figure 10. Mechanism and potential energy diagram of ammonia synthesis on iron.[26] The energies are given in kJ mol^{-1}.

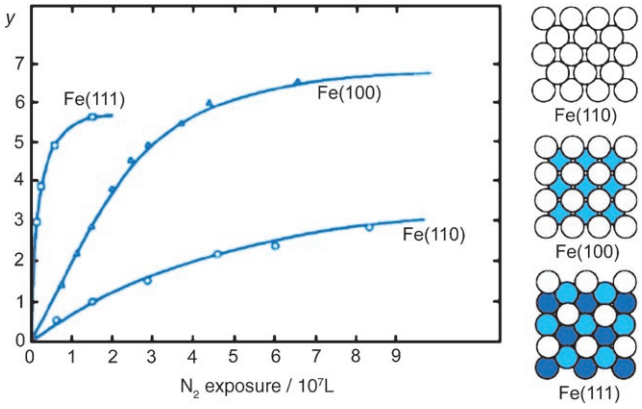

Figure 9. The variation of the relative coverage N atoms (y) chemisorbed at 693 K at various Fe single-crystal surfaces with exposure to gaseous N_2[22] (1 L = 1.33×10^{-6} mbar s is about the exposure that would suffice to form a complete monolayer if each incident molecule is adsorbed).

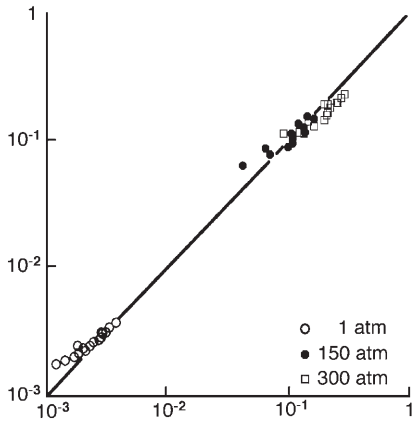

Figure 11. Microkinetics of catalytic ammonia synthesis: Comparison of the yield calculated on the basis of the mechanism presented in Figure 10 (y axis) with experimental data from industrial plants (x axis).[27]

carbon monoxide to carbon dioxide ($2\,CO + O_2 \rightarrow 2\,CO_2$) is the simplest of these reactions and is depicted schematically in Figure 12. The exhaust gas flows through the catalytic converter, where the molecules interact with the surfaces of finely divided metal particles from the platinum group. Thereby the O_2 molecules are dissociatively chemisorbed, and the formed O_{ad} species interact with chemisorbed CO molecules to form CO_2, which is immediately released into the gas phase.

The structures formed by chemisorbed O and CO on a Rh(111) surface are shown as an example in Figure 13:[29] The CO molecules are in this case bonded through the C atom in "on top" positions. They exhibit always the tendency to form densely packed layers, eventually even with occupancy of different adsorption sites[30] (Figure 13a). The O atoms, on the other hand, occupy threefold-coordinated sites and form a rather open mesh of a 2×2 structure (Figure 13b). Since an O_2 molecule in order to become dissociated requires an ensemble of neighboring empty surface atoms, this process will be inhibited as soon as the CO coverage exceeds a certain critical value. The open structure of the O adlayer, on the other hand, still permits adsorption of CO, leading to a mixed phase, as reproduced in Figure 13c, where the two reactants are in close contact and can readily react to form CO_2. Under steady-state flow conditions in a mixture of $O_2 + CO$, the surface of the catalyst will soon be fully covered by adsorbed CO, which prevents oxygen adsorption and hence suppresses the reaction. This problem can only be overcome if the temperature is high enough (≥ 450 K) to enable continuous desorption of part of the adsorbed CO so that gaseous O_2 may compete for these free adsorption sites. (This is the reason why the catalyst of your car does not work in the cold but needs a certain minimum temperature.) The sequence of reaction steps and the energy diagram for this reaction are depicted in Figure 14: After chemisorption of the reactants, $O_{ad} + CO_{ad}$ may react according to the Langmuir–Hinshelwood mechanism[31] by overcoming an activation barrier of 100 kJ mol^{-1} (which is only about half as high at higher coverages[31])—a result that

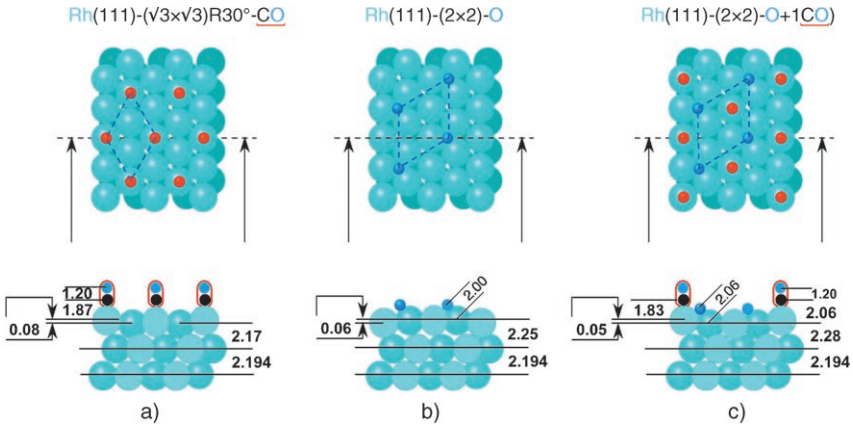

Figure 13. Structures of CO (a), O (b), and O + CO (c) chemisorbed on a Rh(111) surface.[29] Distances are given in Å.

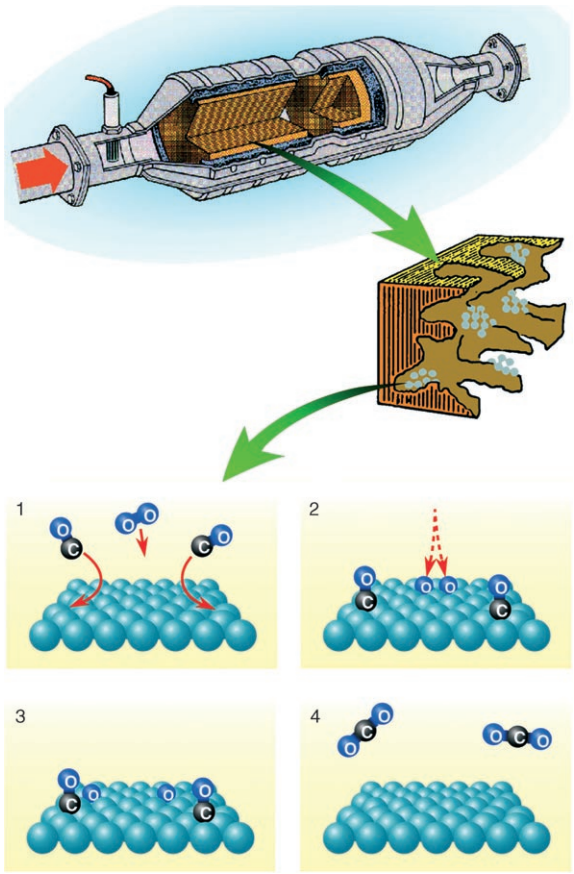

Figure 12. Cartoon illustrating a car exhaust catalyst and the mechanism of CO oxidation.

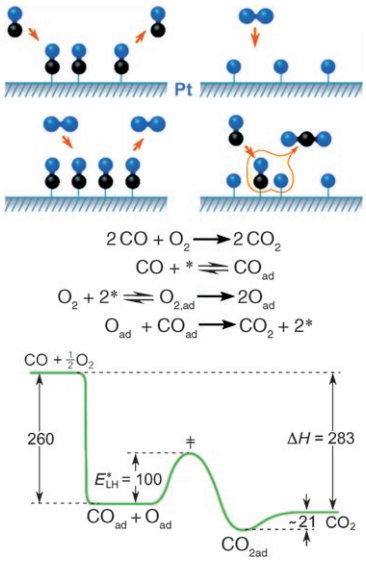

Figure 14. Mechanism and energy diagram for the catalytic oxidation of CO on Pt.

could also be confirmed theoretically on the basis of DFT calculations.[32]

Under steady-state flow conditions, the rate of product formation will usually be constant and a function of the external parameters temperature and partial pressure of O_2 and CO—however, there are exceptions under rare conditions: Already around 1970 it was found in Wicke's laboratory[33] that, for supported Pt catalysts, the rate sometimes exhibits temporal oscillations. Such a situation can also be found with a well-defined Pt(110) surface as shown in Figure 15:[34] At the time marked by an arrow, the O_2 pressure

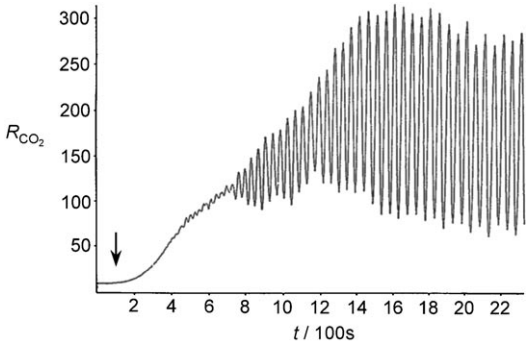

Figure 15. Onset of temporal oscillations of the rate of CO_2 formation on a Pt(110) surface.[34] $T = 470$ K; $p_{CO} = 3 \times 10^{-5}$ mbar.

was raised stepwise from 2.0 to 2.7×10^{-4} mbar. As a consequence the rate slowly increased and then developed periodic variations with eventually constant high amplitudes.

Characteristic for the present system is that it is far away from equilibrium and may develop so-called dissipative structures, as explored in detail by Prigogine (Nobel Prize 1977)[35] and by Haken[36] in the framework of synergetics. A particularly spectacular example for such behavior from population dynamics is reproduced in Figure 16,[37] which shows the variation with time of the number of furs from hares and lynxes delivered to Hudson's Bay Company. The oscillating populations of both species are coupled to each other, with a certain phase shift. The reason seems to be quite obvious: If the lynxes find enough food (= hares) their population grows, while that of the hares decays as soon as their birth rate cannot compensate their loss any more. When the supply of hares drops, the lynxes begin to starve and their population also decays so that that of the hares can recover. The variations of the populations of the two species x and y can be approximately modeled in the language of chemical kinetics in terms of two coupled, nonlinear (ordinary) differential equations (Lotka–Volterra model) as shown in Figure 17 together with their solution for properly chosen parameters α and β. This solution exhibits just the qualitative behavior of the data of Figure 16.

Mathematical description in terms of nonlinear differential equations is essential for these effects, and therefore this field is also denoted as nonlinear dynamics.

With the oscillatory kinetics in the CO oxidation on Pt(110), the situation is still somewhat more complicated. In this case, the reason for this effect has to be primarily sought

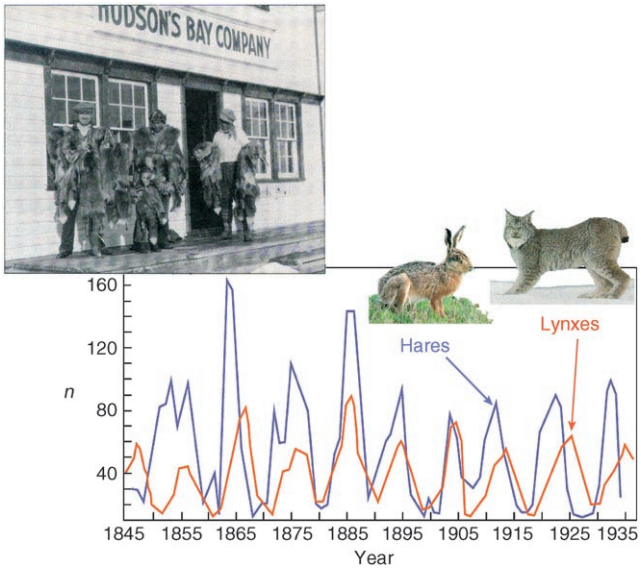

Figure 16. Variation of the number of furs n (in thousands) from hares and lynxes delivered to Hudson's Bay Company with time.[37]

$$\frac{dx}{dt} = \alpha_1 x - \alpha_2 xy, \quad \frac{dy}{dt} = \beta_1 xy - \beta_2 y$$

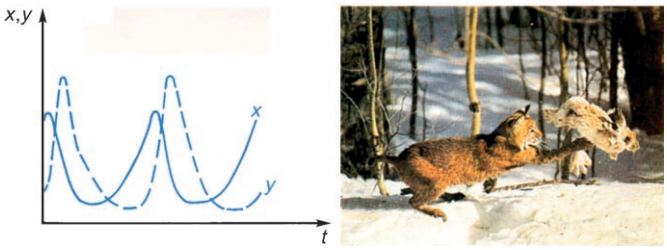

Figure 17. The Lotka–Volterra model describing the observation in Figure 16.

in the structure of the Pt(110) surface and its transformation under the influence of adsorbates. As already recognized by Langmuir:[38] "*The atoms in the surface of a crystal must tend to arrange themselves so that the total energy will be a minimum. In general, this will involve a shifting of the positions of the atoms with respect to each other.*"

Such a reconstruction is exhibited by the clean Pt(110) surface.[39] Instead of the termination by the corresponding bulk crystal plane (Figure 18b: 1×1 structure), every second

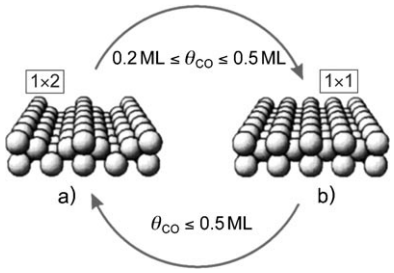

Figure 18. Structures of the Pt(110) surface:[39] a) the 1×2 structure of the clean surface; b) the 1×1 structure representing termination of the bulk structure.

row along the [1$\bar{1}$0] direction is missing, giving rise to a 1 × 2 structure (Figure 18a). In this way, small facets with (111) orientation are exposed, leading to a lower energy than with the 1 × 1 phase. The two phases differ also with respect to their adsorption properties: Chemisorption of CO is accompanied by a higher adsorption energy on the 1 × 1 phase than on the 1 × 2 structure, so that local 1 × 2 → 1 × 1 transformation takes place as soon as the CO coverage exceeds a value of 0.2 monolayers (ML).[40] On the other hand, the sticking coefficient for dissociative oxygen coverage on the 1 × 1 phase exceeds that on the 1 × 2 phase by about 50 %.[41] The occurrence of temporal oscillations in the rate of CO_2 can now be rationalized as follows: If a clean Pt(110) surface (1 × 2) is exposed to a proper mixture of $CO + O_2$, adsorption of CO will suffice to cause local 1 × 2 → 1 × 1 transformation. On the newly created 1 × 1 patches, the oxygen sticking coefficient will be higher, so that a higher O coverage will be built up, giving rise to an enhanced production of CO_2. By this latter process, the excess CO will be consumed so that the surface structure transforms back from 1 × 1 to 1 × 2, and one cycle is completed. Mathematical modeling requires in this case three variables, the coverages of O and CO, and the fraction of the surface present as the 1 × 1 phase. Solution of the resulting three coupled nonlinear differential equations for properly chosen parameters is shown in Figure 19 and reproduces the experimental findings.[42]

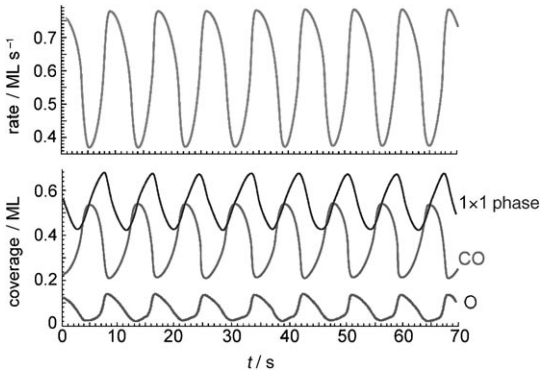

Figure 19. Theoretical description of the oscillatory kinetics of CO oxidation on a Pt(110) surface.[42] $T = 540$ K; $p_{O_2} = 6.7 \times 10^{-5}$ mbar; $p_{CO} = 3 \times 10^{-5}$ mbar.

However, so far the story is still incomplete: If the elements of an extended system exhibit temporal oscillations as a whole, some kind of lateral coupling between these elements is required in order to achieve synchronization. As a consequence of these considerations, the state variables (i.e. the surface concentrations of the adsorbates x_i) are in general not only dependent on time t but also on the spatial coordinates r_i. As summarized in Figure 20, coupling between different regions on the surface is achieved by transport processes. If the heat capacity of the catalyst is low enough, spots with surface concentrations favoring higher reaction rates will also attain higher local temperature as a result of the exothermicity of the overall reaction, and then heat conduction across the catalyst surface will provide coupling between different parts. Such a situation will usually be found with oscillatory kinetics on supported catalysts under high-pressure conditions,[43] but has also been studied in detail with a very thin (ca. 200 nm) Pt(110) single-crystal foil, where periodic variation of the reaction rate caused corresponding changes of the temperature. The latter effect initiated varying thermal expansion and hence deformation, which was denoted as "heartbeats of a catalyst".[44]

Lateral variation of state variables (surface concentrations) x_i

Coupling between different parts of the surface by

- **Diffusion**
- **Heat conductance**
- **Variation of partial pressures**
- **Electric field**

Reaction-diffusion systems: $\frac{\partial x_i}{\partial t} = F_i(x_j, p_k) + D_i \nabla^2 x_i$

Figure 20. Spatio–temporal self-organization in open systems far from equilibrium.

Under isothermal conditions at low pressures, local differences of the surface concentrations cause surface diffusion of the adsorbates, and a mathematical description can now be obtained in terms of reaction-diffusion equations, that is, a set of coupled nonlinear partial differential equations combining the kinetics with the diffusion of the adsorbed species (Figure 20). The length scale of the resulting spatio–temporal concentration patterns is no longer governed by atomic dimensions but by the so-called diffusion length, which in our case is of the order of some tens of micrometers.[45] These patterns were imaged by the technique of photoemission electron microscopy (PEEM):[46] Adsorbed O and CO species are accompanied by different electric dipole moments and hence different work function changes, which in turn give rise to varying intensities of photoemitted electrons. Dark areas in the images are essentially O-covered while brighter patches are CO-covered. As an example, Figure 21 shows so-called target patterns, concentric elliptic features propagating preferentially along the [1$\bar{1}$0] direction of the Pt(110) surface (where CO diffusion is faster than along the

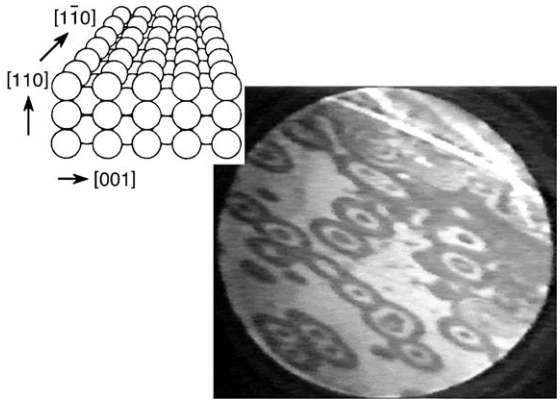

Figure 21. Target patterns in catalytic oxidation of CO on a Pt(110) surface as imaged by PEEM.[47] A real-time movie showing the pattern changes is presented in the Supporting Information.

[001] direction) on a background changing periodically between bright (= CO-covered) and dark (= O-covered), while the external parameters of temperature and partial pressures are kept constant as indicated.[47]

Under other external parameters, typical spiral waves as shown in Figure 22 develop and propagate with front speeds of a few $\mu m\,s^{-1}$. The core of a spiral is often formed by a region on the surface with enhanced defect density, and this effect is also responsible for the fact that the wavelengths of the spiral waves vary to some extent.[48]

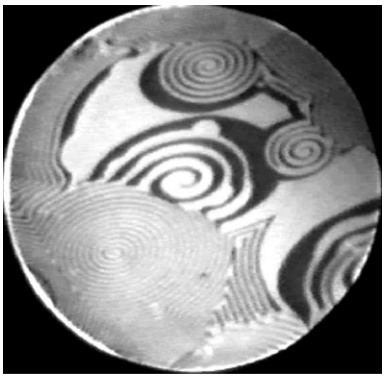

Figure 22. PEEM image of the formation of spiral waves in catalytic CO oxidation on a Pt(110) surface.[48] $T = 448$ K; $p_{O_2} = 4\times10^{-4}$ mbar; $p_{CO} = 4.3\times10^{-5}$ mbar. The diameter of the picture is 500 μm. A real-time movie showing the pattern changes is presented in the Supporting Information.

Since the mechanism of this reaction and all its parameters are well established experimentally, these data may also be used to simulate the resulting patterns by numerical solution of the underlying differential equations. This is shown in Figure 23 for the case of spiral wave development.[49] If the parameters are changed slightly, the solution no longer exhibits regular spirals, but they break up to form spiral turbulence or spatio–temporal chaos (Figure 24). Experimental verification of such a situation is demonstrated by Figure 25.

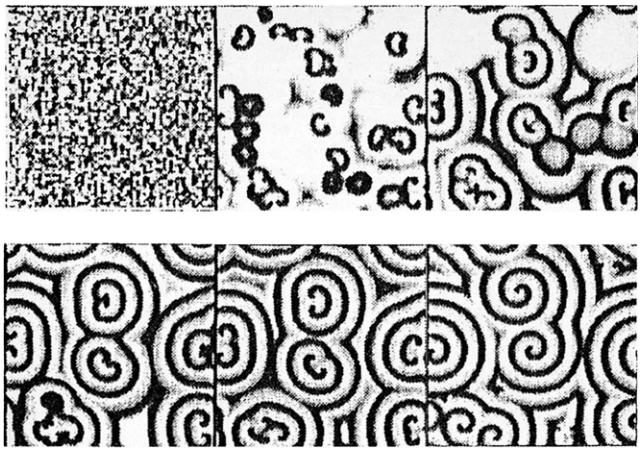

Figure 23. Computer simulation of the evolution of spiral waves in catalytic CO oxidation.[49]

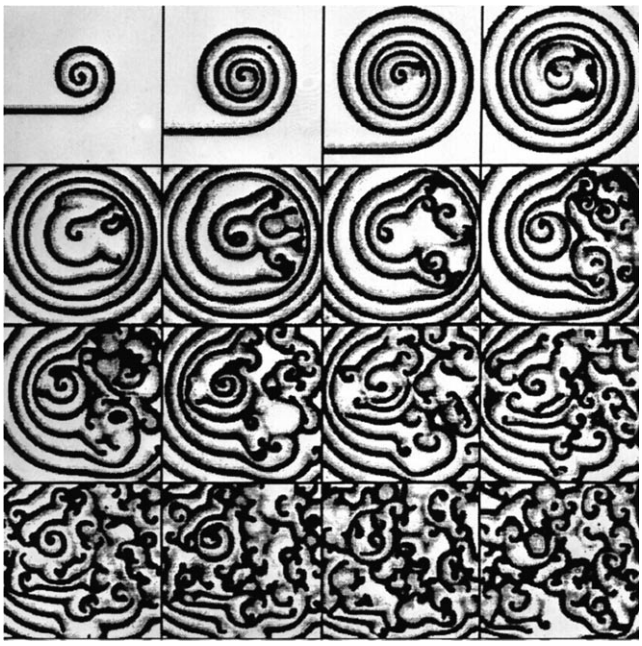

Figure 24. Computer simulation of the break up of spiral waves to chemical turbulence.

Figure 25. PEEM image from a Pt(110) surface in the state of chemical turbulence. $T = 548$ K; $p_{O_2} = 4\times10^{-4}$ mbar; $p_{CO} = 1.2\times10^{-4}$ mbar. The image size is 360×360 μm. A real-time movie showing the pattern changes is presented in the Supporting Information.

We have now reached a state in which a system that in principle is very simple—a chemical reaction between two diatomic molecules on a well-defined single-crystal surface with fixed external parameters and for which all individual reaction steps are known—nevertheless exhibits rather complex behavior. Such effects are generally expected for open systems far from equilibrium and are hence believed to govern also processes in nature. Our system can be considered to be a rather simple model for studying these types of phenomena. One might for example be interested to modify pattern formation from outside by affecting one of the control parameters. This can be done either locally be heating a small spot on the surface by laser light[50] or globally by a feedback mechanism in which the actual reaction rate (or integral coverage of one of the surface species) is used to regulate the flow of one of the reacting gases.[51] A series of patterns

created in this way from a turbulent initial state by different strength and delay of the feedback is reproduced in Figure 26. These patterns are reminiscent of similar phenomena found in nature (Figure 27), but also of Vincent van Gogh's vision of our world in his painting *The Starry Night* (Figure 28).

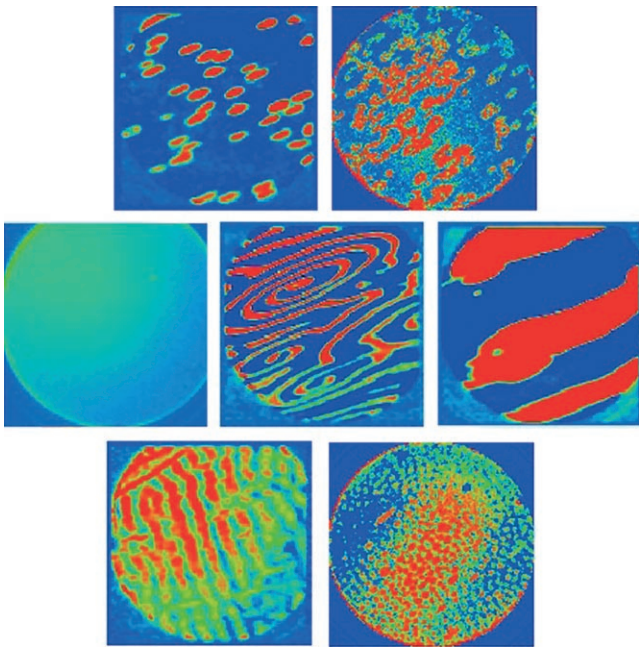

Figure 26. Transformation of a state of spiral turbulence into other different patterns by a feedback mechanism with different strength and delay of the feedback.[51]

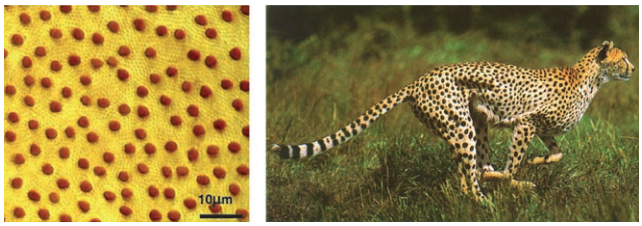

Figure 27. Phenomena of pattern formation found in nature: the structure of the retina and leopard fur.

Figure 28. Vincent van Gogh's painting *The Starry Night*.

4. Conclusions

This is no review article but more a brief account for a broader audience of some of the work that had been considered to be the basis for the awarding of the Nobel Prize. Numerous co-workers were involved in our continuing attempt to understand how chemical reactions on solid surfaces take place. Without their efforts, the results presented herein could not have been achieved, and therefore I am heartily grateful to all of them. Their names as well as a complete bibliography up to 2004 can be found in a recent special issue of the *Journal of Physical Chemistry B*.[52]

Received: January 30, 2008
Published online: March 20, 2008

[1] *Briefwechsel zwischen Goethe und Johann Wolfgang Döbereiner (1810–1830)* (Ed.: J. Schiff), **1994**, p. 78 Published in: J. W. Döbereiner, *Schweigg. J.* **1823**, *39*, 1.
[2] J. J. Berzelius, *Jber. Chem.* **1835**, *15*, 237 (submitted to the academy on March 31, 1835).
[3] G. Ertl, T. Gloyna, *Z. Phys. Chem.* **2003**, *217*, 1207.
[4] W. Ostwald, *Phys. Z.* **1902**, *3*, 313; W. Ostwald, *Ann. Naturphil.* **1910**, *9*, 1.
[5] W. Crookes, Rep. of the 68th meeting of the British Association for the Advancement of Science Bristol 1898, John Murray, London, **1898**, p. 3 Quoted in S. A. Topham, *Catalysis, Science and Technology, Vol. 7* (Eds.: J. R. Anderson, M. Boudart), Springer, Berlin, **1955**, p. 1.
[6] F. Haber, *Z. Elektrochem.* **1910**, *16*, 244; F. Haber, R. Le Rossignol, *Z. Elektrochem.* **1913**, *19*, 53.
[7] W. Appl, *Ammonia*, Wiley-VCH, Weinheim, **1999**.
[8] A. Mittasch, *Geschichte der Ammoniak-Synthese*, Verlag Chemie, Weinheim, **1957**.
[9] P. H. Emmett in *The Physical Basis for Heterogeneous Catalysis* (Eds.: R. I. Jaffee, E. Drauglis), Plenum, New York, **1975**, p. 3.
[10] G. Ertl, D. Prigge, R. Schlögl, D. Weiss, *J. Catal.* **1983**, *79*, 359.
[11] I. Langmuir, *Trans. Faraday Soc.* **1922**, *17*, 607.
[12] a) G. Ertl, J. Küppers, *Low Energy Electrons and Surface Chemistry*, 2nd ed., VCH, Weinheim, **1985**; b) D. P. Woodruff, T. A. Delchar, *Modern Techniques of Surface Science*, Cambridge University Press, Cambridge, **1994**; c) J. C. Vickerman, *Surface Analysis*: *The Principal Techniques*, Wiley, New York, **1997**; d) K. W. Kolasinski, *Surface Science. Foundations of Catalysis and Nanoscience*, Wiley, New York, **2002**.
[13] J. E. Lennard-Jones, *Trans. Faraday Soc.* **1932**, *28*, 333.
[14] a) G. Ertl, *Adv. Catal.* **2000**, *45*, 1; b) A. C. Luntz in *Chemical Bonding at Surfaces and Interfaces* (Eds.: A. Nilsson, L. G. M. Petterson, J. K. Nørskov), Elsevier, Dordrecht, **2008**, p. 143.
[15] J. Wintterlin, R. Schuster, G. Ertl, *Phys. Rev. Lett.* **1996**, *77*, 123.
[16] G. Ertl, *J. Vac. Sci. Technol.* **1977**, *14*, 435.
[17] a) S. Funk, M. Bonn, D. N. Denzler, C. Hess, M. Wolf, G. Ertl, *J. Chem. Phys.* **2000**, *112*, 9888; b) M. Bonn, S. Funk, C. Hess, D. N. Denzler, C. Stampfl, M. Scheffler, M. Wolf, G. Ertl, *Science* **1999**, *285*, 1042.
[18] J. Wintterlin, J. Trost, S. Renisch, R. Schuster, T. Zambelli, G. Ertl, *Surf. Sci.* **1997**, *394*, 159.
[19] S. Renisch, R. Schuster, J. Wintterlin, G. Ertl, *Phys. Rev. Lett.* **1999**, *82*, 3839.
[20] T. Zambelli, J. Trost, J. Wintterlin, G. Ertl, *Phys. Rev. Lett.* **1996**, *76*, 795.
[21] R. Imbihl, R. J. Behm, G. Ertl, W. Moritz, *Surf. Sci.* **1982**, *123*, 129.

[22] F. Boszo, G. Ertl, M. Grunze, M. Weiss, *J. Catal.* **1977**, *49*, 18; F. Boszo, G. Ertl, M. Grunze, M. Weiss, *J. Catal.* **1977**, *50*, 519.
[23] a) G. Ertl in *Encyclopedia of Catalysis*, *Vol. 1* (Eds.: J. T. Hervath, E. Iglesia, M. T. Klein, J. A. Lercher, A. J. Russell, G. I. Stiefel), Wiley, New York, **2003**, p. 329; b) R. Schlögl in *Handbook of Heterogeneous Catalysis*, 2nd ed. (Eds.: G. Ertl, H. Knözinger, F. Schüth, J. Weitkamp), Wiley-VCH, Weinheim, **2008**, chap. 12.1.
[24] G. Ertl, M. Weiss, S. Lee, *Chem. Phys. Lett.* **1979**, *60*, 391.
[25] N. D. Spencer, R. C. Schoonmaker, G. A. Somorjai, *J. Catal.* **1982**, *74*, 129.
[26] G. Ertl, *Catal. Rev. Sci. Eng.* **1980**, *21*, 201.
[27] P. Stoltze, J. K. Nørskov, *Phys. Rev. Lett.* **1985**, *55*, 2502; P. Stoltze, J. K. Nørskov, *J. Catal.* **1988**, *110*, 1.
[28] a) M. Bowker, I. B. Parker, K. C. Waugh, *Appl. Catal.* **1985**, *14*, 101; b) J. A. Dumesic, A. A. Trevino, *J. Catal.* **1989**, *116*, 119; c) *Topics in Catalysis*, *Vol. 1* (Eds.: H. Topsoe, M. Boudart, J. K. Topsoe), Springer, Heidelberg, **1994**.
[29] S. Schwegmann, H. Over, V. De Renzi, G. Ertl, *Surf. Sci.* **1997**, *375*, 91.
[30] A. Föhlisch, M. Nyberg, J. Hasselström, O. Varis, L. G. M. Petterson, A. Nilsson, *Phys. Rev. Lett.* **2000**, *85*, 3309.
[31] a) C. N. Hinshelwood (Nobel Prize 1956), *The Kinetics of Chemical Change*, Clarendon Press, Oxford, **1940**; b) J. Wintterlin, S. Völkening, T. V. W. Janssens, T. Zambelli, G. Ertl, *Science* **1997**, *278*, 1931.
[32] T. Kuri, P. Hu, T. Deutsch, P. L. Silvestrelli, J. Hutter, *Phys. Rev. Lett.* **1998**, *80*, 650.
[33] a) P. Hugo, *Ber. Bunsen-Ges.* **1970**, *74*, 121; b) H. Beusch, D. Fieguth, E. Wicke, *Chem. Ing. Tech.* **1972**, *15*, 445.
[34] M. Eiswirth, G. Ertl, *Surf. Sci.* **1986**, *177*, 90.
[35] G. Nicolis, I. Prigogine, *Self-Organization in Non-Equilibrium Systems*, Wiley, New York, **1977**.
[36] a) H. Haken, *Synergetics, an Introduction*, Springer, Heidelberg, **1977**; b) A. S. Mikhailov, *Foundations of Synergetics*, *Vol. I* and *II*, Springer, Heidelberg, **1991**.
[37] D. A. McLulich, *Variations in the Number of Varying Hare*, University of Toronto Press, Toronto, **1937** (after ref. [36a]).
[38] I. Langmuir, *J. Am. Chem. Soc.* **1916**, *38*, 1221.
[39] a) S. R. Bare, P. Hoffmann, D. A. King, *Surf. Sci.* **1984**, *144*, 347; b) T. E. Jackman, J. A. Davies, D. P. Jackson, W. N. Unertl, P. R. Norton, *Surf. Sci.* **1982**, *120*, 389.
[40] T. Gritsch, D. Coulman, R. J. Behm, G. Ertl, *Phys. Rev. Lett.* **1989**, *63*, 1086.
[41] N. Freyer, M. Kiskinova, D. Pirug, H. P. Bonzel, *Surf. Sci.* **1986**, *166*, 206.
[42] K. Krischer, M. Eiswirth, G. Ertl, *J. Chem. Phys.* **1992**, *96*, 9161.
[43] M. M. Slinko, N. Jaeger, *Oscillating Heterogeneous Catalytic Systems*, Elsevier, Dordrecht, **1994**.
[44] F. Cirak, J. E. Cisternas, A. M. Cuitino, G. Ertl, P. Holmes, Y. Kevrekidis, M. Oritiz, H. H. Rotermund, M. Schunack, J. Wolff, *Science* **2003**, *300*, 1932.
[45] a) G. Ertl, *Science* **1991**, *254*, 1750; b) R. Imbihl, G. Ertl, *Chem. Rev.* **1995**, *95*, 697.
[46] W. Engel, M. Kordesch, H. H. Rotermund, S. Kubala, A. von Oertzen, *Ultramicroscopy* **1991**, *9*, 6162.
[47] S. Jakubith, H. H. Rotermund, W. Engel, A. von Oertzen, G. Ertl, *Phys. Rev. Lett.* **1990**, *65*, 3013.
[48] S. Nettesheim, A. von Oertzen, H. H. Rotermund, G. Ertl, *J. Chem. Phys.* **1993**, *98*, 9977.
[49] M. Bär, N. Gottschalk, M. Eiswirth, G. Ertl, *J. Chem. Phys.* **1994**, *100*, 1202.
[50] J. Wolff, A. G. Papathanasiou, Y. Kevrekidis, H. H. Rotermund, G. Ertl, *Science* **2001**, *294*, 134.
[51] M. Kim, M. Bertram, M. Pollmann, A. von Oertzen, A. S. Mikhailov, H. H. Rotermund, G. Ertl, *Science* **2001**, *292*, 1357.
[52] Special issue: *J. Phys. Chem. B* **2004**, *108*, 14183–14788.